HHS Public Access

Author manuscript

J Electrocardiol. Author manuscript; available in PMC 2018 May 01.

Published in final edited form as:

J Electrocardiol. 2017 ; 50(3): 342–348. doi:10.1016/j.jelectrocard.2016.12.005.

Optimal Configuration of Adhesive ECG Patches suitable for Long-term Monitoring of a Vectorcardiogram

Muammar M. Kabir, PhD, **Erick A. Perez-Alday, PhD**, **Jason Thomas, BS**, **Golriz Sedaghat, BS**, and **Larisa G. Tereshchenko, MD, PhD**

Knight Cardiovascular Institute, Oregon Health and Science University, Portland, USA

Abstract

The purpose of this study was to develop optimal configuration of adhesive ECG patches placement on the torso, which would provide the best agreement with the Frank orthogonal ECGs. Ten seconds of orthogonal ECG followed by 3–5 minutes of ECGs using patches at 5 different locations simultaneously on the torso were recorded in 50 participants at rest in sitting position. Median beat was generated for each ECG and 3 patch ECGs that best correlate with orthogonal ECGs were selected for each participant. For agreement analysis, spatial QRS-T angle, spatial QRS and T vector characteristics, spatial ventricular gradient, roundness, thickness and planarity of vectorcardiographic (VCG) loops were measured. Key VCG parameters showed high agreement in Bland-Altman analysis (spatial QRS-T angle on 3-patch ECG vs. Frank ECG bias 0.3 (95% limits of agreement [−6.23;5.71 degrees]), Lin's concordance coefficient=0.996). In conclusion, newly developed orthogonal 3-patch ECG can be used for long-term VCG monitoring.

Keywords

ECG patch; vectorcardiogram; QRS-T angle

Introduction

Heart disease is the leading cause of death in the United States[1]. The Electrocardiogram (ECG) is a widely used non-invasive tool for risk stratification and diagnosis of several cardiovascular diseases. For example, atrial fibrillation (AF) is a common clinical arrhythmia which is estimated to affect 2.7–6.1 million people in the US and is expected to double by 2050[2]. Long-term ECG monitoring is an important diagnostic tool for asymptomatic and infrequent cardiac arrhythmias. Recently developed, wearable adhesive ECG patches have revolutionized long-term ECG monitoring. Lightweight compact ECG patches are comfortable to wear, therefore reducing barriers to patient compliance. It has been shown that the longer duration of ambulatory ECG monitoring the higher diagnostic

Corresponding Author: Larisa G. Tereshchenko, Knight Cardiovascular Institute, Oregon Health and Science University, Portland, OR 97239, USA, Tel: +1 503-494-2374, tereshch@ohsu.edu.

yield[3–5]. However, single lead ECG patch monitoring has obvious limitations: difficulties in discrimination between cardiac beat and artefact, and limited capabilities in diagnosing ischemia or origin of cardiac arrhythmias.

The vectorcardiogram (VCG), which was first constructed in 1920 by Mann[6] and defined in 1938 by Wilson[7], represents movement of heart vector in three orthogonal dimensions. Analysis of VCG can provide complementary information to the 12-lead ECG and has been demonstrated to help define abnormal electrophysiological substrate in patients with life-threatening ventricular arrhythmias and sudden cardiac death (SCD)[8,9]. Recently we showed that VCG measures of global electrical heterogeneity such as spatial QRS-T angle, sum absolute QRST integral (SAI QRST), and spatial ventricular gradient (SVG) are associated with risk for sudden cardiac death (SCD)[10]. It is well known that the risk of SCD is dynamic. However, previously there were no tools for long-term VCG monitoring.

The BioStamp Research Connect™ (MC10, Inc., Lexington, MA) patch is a newly developed mobile telemetry device for continuous recording of high resolution (up to 1000 Hz) ECG and electromyographic signals, and body movements, based on epidermal electronics technology[11]. The goal of this study was to develop the optimal configuration of patch placement on the torso which would provide the best agreement with the modified Frank orthogonal ECG. We hypothesized that patches placed in locations looking at the heart from three orthogonal axes around the heart's centre would provide an ECG with information similar to the orthogonal ECG.

Methods

Study population

We conducted a cross-sectional study at Oregon Health and Science University (OHSU). The study conformed to principles outlined in the Declaration of Helsinki and was approved by the OHSU Institutional Review Board. Individuals free from any known skin allergies were enrolled in this study. All participants provided written informed consent.

Electrocardiogram Recording

The protocol included 10 seconds of modified Frank orthogonal XYZ ECG recording followed by 3–5 minutes of five simultaneous single lead ECG recordings from 5 different locations on the torso around the heart at rest in a sitting position. The Orthogonal ECGs were digitally acquired at a sampling rate of 500 Hz using the MAC 5500 ECG system (Marquette Electronics, Milwaukee, WI, USA). Single lead ECGs sampled at 500 Hz were obtained using BioStamp Research Connect™ patches (MC10, Lexington, MA, USA) applied at the following 5 locations (Figure 1): P1 is placed horizontally in the 3rd intercostal space between the left parasternal and mid-clavicular line; P2 is placed horizontally in the 5th intercostal space between the left parasternal and mid-clavicular lines; P3 is placed vertically at left parasternal line in the 4th intercostal space; P4 is placed at the horizontal level of P2 at the left anterior axillary line; P5 is placed at the horizontal level of P2 at the left mid-axillary line. A Samsung Galaxy tablet was used to assign patches for each subject,

start and stop recordings for each sensor, and transfer ECG patch raw signal data to the cloud for storage and subsequent analysis.

ECG and VCG Data analysis

Custom written software developed using Matlab (MathWorks, Natick, MA, USA) was used for data analysis. Orthogonal XYZ ECGs obtained from MAC 5500 were processed with the GE Magellan research utility (GE Marquette, Milwaukee, WI) to obtain median orthogonal ECGs. For each of the ECG Patch recordings a singular clean (artefact-free, noise-free), simultaneous, 10 second ECG Patch segment with all consecutive sinus beats was selected from all patches and a median beat for each recording was generated. Secondly, the gains of the median beat ECGs from patches for each participant were adjusted by multiplying by a constant coefficient (range: $1x10^6$ to $3.3x10^6$) to match the median orthogonal ECGs. Thirdly, for each participant, median beats from all the five ECG patches were compared using correlation analysis against each orthogonal X-, Y-, and Z-lead ECGs. Lastly, the median beats of 3 patches with the highest Pearson's correlation coefficient were selected for further analysis (Figure 2A). There were no overlaps in patch selection for representation of orthogonal X-, Y-, or Z-leads in any participant.

For analysis of agreement, the spatial mean and peak QRS-T angle, azimuth and elevation of mean and peak QRS, T and spatial ventricular gradient (SVG) vectors, and sum of absolute integral (SAI) QRST were measured on VCGs constructed from orthogonal ECGs and ECGs obtained from patches. The mean spatial QRS-T angle was measured as the angle between the 3-dimensional mean QRS and T vectors, calculated as the vector sum from onset to offset of QRS and T vectors respectively, as described previously[10]. For the calculation of peak spatial QRS-T angle, the peak QRS and T vectors were defined as the vectors from the origin to the furthest point on the QRS and T loops respectively, as described previously[12]. The X, Y and Z components of the SVG vector were calculated as the integration of the area covered from the beginning of the QRS complex to the end of the T wave in the X, Y and Z axes[10]. SAI QRST was measured as the arithmetic sum of the areas under the entire QRS-T curve, as described previously[13,14].

Furthermore, the following VCG parameters were calculated as described in our previous study[15]: VCG roundness, thickness and planarity. In short, the roundness index was measured as the ratio of the QRS or T loop to the square of the QRS or T peak vector[16]. The thickness was measured by calculating the distance between two parallel planes encompassing the horizontal QRS or T loop. the QRS loop planarity index was calculated as the ratio of the magnitude of geometrical area vector to the area of the entire QRS loop[17].

Statistical analysis

Data were analysed using STATA 13 (StataCorp LP, College Station, TX, USA). Bradley-Blackwood test (which simultaneously compares the means and variances of two measurements), Lin's concordance correlation coefficient and Bland-Altman analysis[18] was used for the assessment of agreement of VCG parameters obtained from modified Frank orthogonal ECGs and newly developed orthogonal 3-patch ECGs. Results are presented as mean ± standard deviation. A P-value of <0.05 was considered significant.

Results

Study population

Data of 50 study participants were analysed (mean age: 38.9±14.6 yrs; 24 (48%) female and 38 (76%) white). Clinical characteristics of the participants are given in Table 1.

Optimal configuration of ECG patches' placement

The best-matching ECG-patch X lead strongly correlated with orthogonal X lead (0.91±0.03); ECG-patch Y lead strongly correlated with orthogonal Y lead (0.91±0.04); ECG-patch Z lead strongly correlated with orthogonal Z lead (0.91±0.03). We observed a significant difference in the choice of the best X lead between healthy study participants (P1 in 69%) and participants with the history of cardiovascular disease (P2 in 75%); P=0.019. Patch P3 showed the strongest correlation with orthogonal Y lead in 80% of participants with cardiovascular disease, whereas in healthy participants placement of ECG patch correlating with Y lead was less important: "the best Y-lead" configuration was nearly evenly distributed across patches P2 (55%) and P3 (45%). Similarly, in 75% of participants with cardiovascular disease the "best Z-lead" corresponded to P5, whereas both locations (P4 in 58% and P5 in 42%) had the strongest correlation with orthogonal Z-lead in healthy participants (P=0.093). There was no significant effect of age, sex, race or ethnicity on the best configuration of placement of patches. Required adjustment of gain inversely correlated with the strength of correlation of the "best Z ECG patch lead" with orthogonal Z-lead ($r = -0.282$; P=0.047).

Agreement of spatial QRS-T angle, azimuth and elevation of QRS, T and SVG vectors

Both mean and peak QRS-T angles showed a very high agreement when comparing ECG recordings using the orthogonal lead system to ECG patches (Table 2). The azimuth and elevation of all the mean and peak QRS, T and SVG vectors, and SAI QRST also showed a strong agreement when comparing the recorded with the reconstructed orthogonal ECGs (Table 2).

A high agreement was observed in the calculated thicknesses of the QRS and T loops constructed from patch ECGs and those obtained from orthogonal ECGs. However, the roundness and planarity indices showed lower agreement between the VCGs for modified Frank and patch.

Discussion

In this study we reconstructed VCG and orthogonal ECG using the newly available BioStamp Research Connect^{TM} (MC10, Inc., Lexington, MA) ECG patches. We demonstrated that placing 3 single-lead ECG patches in orthogonal position around the electrical center of the heart (Figure 1B) can give us results similar to modified Frank orthogonal ECGs.

Electronic systems with physical properties matched to the skin or epidermis that can be used to improve non-invasive electrophysiological recordings have been of interest. These electronic devices configured for measuring ECG on the chest surface revealed high-quality

signals containing information on the phases of heartbeat, rapid depolarization and repolarization of cardiac waves[11,19,20]. The BioStamp Research Connect™ (MC10, Inc., Lexington, MA) is a single-lead, light-weight ambulatory ECG, EMG and body movement adhesive patch monitor that can acquire, store and send data to the cloud from where they can be monitored and retrieved for analysis. The simple wireless design and flexibility of the patch along with its water-resistant properties make it easier for participants to do their daily activities with minimal to no disruption. The ECG patch has the ability to acquire high resolution (up to 1 kHz) signals thus allowing for reliable study of beat to beat variabilities[21]

From the lead field theory[22–24], voltage measured in a specific lead can be defined as the dot product of the vectors characterizing the electrical activity of the heart and the lead where the ECG is recorded, as if a unit current was injected in the lead terminals[25,26]. Therefore, for an ideal orthonormal measurement of the electric heart vector, three things are required: a) the three components of the electric heart vector form an orthogonal system and the orthogonal lead vectors are parallel to the orthogonal coordinated axes; b) each orthogonal lead field is uniform throughout the heart; c) all the three orthogonal heart vector components are detected with the same sensitivity(to ensure comparable magnitude)[27]. Frank emphasized that the electrodes should be placed at a level corresponding to the electrical center of the heart[28,29]. McFee and Parungao placed electrodes in the form of an equilateral triangle such that the electrodes are at a distance of 6cm from the center of the triangle located at the fifth intercostal space, 2cm to the left of the sternal margin[30]. This configuration produces uniform lead fields in the region of the heart. Importantly, the assumptions of the ECG lead theory are not very restrictive and allow the theory to be formulated for any conceivable ECG lead. The lead vector of an ECG patch can be characterized as the potential difference between the patch electrodes. The patch electrodes are closely spaced with a narrow lead field and hence are very sensitive to slight variations in the location of a patch. Placing the patches in an orthogonal configuration with its center similar to the Frank ECG system and approximately at the electrical center of the heart would thus generate a lead field with sufficient homogeneity and ensure that the lead vector variation throughout the heart is as uniform as possible. In other words, the patches provide a projection (though smaller in magnitude) of each modified Frank orthogonal lead vector. In our study we corrected voltage by 10^6 to account for this difference. Consequently, all our calculated VCG parameters - except for roundness and planarity - obtained from patch ECGs showed a strong agreement with those obtained from orthogonal ECGs. Likely explanation of a low agreement in roundness and planarity is a non-uniformity of the lead field formed by closely-spaced electrodes of ECG patch. Remarkably, in this study spatial vectors (QRS, T, and SVG) measured on orthogonal patch-ECG demonstrated high agreement with spatial vectors measured on VCG using modified Frank orthogonal ECG. This finding opens opportunity for long-term monitoring of global electrical heterogeneity measures (spatial QRS-T angle, SVG and SAI QRST) and further study dynamic risk of sudden cardiac death[10].

A difference in placement of ECG patches between healthy individuals and patients with history of cardiovascular disease was observed. We used identical patches (one standard electrode size and inter-electrode distance) in all study participants. Thus, there was no difference in the lead field between study participants. However, due to the differences in the

size and the location/position of the heart in the torso, narrow lead field of the patch likely probed slightly different regions of the heart in different patients. Ideally, the patches should be placed such that they form an orthogonal system with the center in the electrical center of the heart. As compared to healthy individuals, the electrical center of the heart in cardiovascular patients is shifted due to enlarged hearts and hence the placement of patches differed between the two groups.

This study has significant clinical importance. Prolonged adhesive patch monitors demonstrated increased arrhythmia diagnostic yield as compared with conventional 24–48 hours of Holter monitoring[31]. The data from the patches can be used to reliably extract vital ECG and VCG characteristics, and study clinical arrhythmias, ECG abnormalities and beat-to-beat variations in high risk patients. Furthermore, in the presence of factors such as changes in body position and respiration which affect patch ECGs, a 3-lead ECG patches' configuration can provide more accurate measurement and beat discrimination compared to a single-lead ECG. Previous studies emphasized on multi-lead ECG recording due to several advantages: onset and offset measurement of waveforms are more accurate[32]; spatial vector magnitude can be created from multi-lead which may provide better determination of fiducial points[32]; improve the reliability of ECG-derived respiration[33]; and reduce the influence of the mechanical effect of respiration on the T-wave end location using multi-lead delineation[34]. Based on our study results, we recommend the following protocol for long-term VCG monitoring and analysis. For highest accuracy it is recommended to first record a 10 second orthogonal Frank ECGs, and then adjust the position of patches around our suggested location (Figure 1B) that provide ECGs (as viewed in real-time on the tablet) comparable to orthogonal ECGs. Inter-individual variation in the location of the electrical center of the heart can affect the properties of the recorded ECG signals. At the same time three ECG patches could be placed such that they form orthogonal triangle around the presumed heart's electrical center as shown in Figure 1B. However, using the same location for placement of patches in all participants might reduce the accuracy of results. Due to limitations in the regional abnormalities (e.g. local ischemia) assessment by the narrow lead field, it is important to emphasize that patch ECGs recorded with torso placement of the electrodes should not be used interchangeably with standard 12-lead ECGs for serial comparison.

Limitations

The study population mostly consisted of healthy individuals. The optimal position of patches recommended in this study needs to be tested on a larger population of patients with cardiac abnormalities.

Conclusion

This study demonstrated feasibility and developed an optimal configuration of adhesive ECG patches for continuous monitoring of orthogonal ECGs similar to orthogonal Frank ECGs. The patches can be used for monitoring of long-term VCG parameters such as QRS-T angle, spatial QRS and T vector characteristics, and other global electrical heterogeneity

parameters. Results of the study for the first time open avenue for long-term VCG monitoring.

Acknowledgments

The authors would like to thank all the study participants. This work was supported in part by R01HL118277 (LGT).

References

1. Mozaffarian, D., Benjamin, EJ., Go, AS., Arnett, DK., Blaha, MJ., Cushman, M., et al. A Report From the American Heart Association. 2015. Heart Disease and Stroke Statistics—2016 Update.
2. Go AS, Hylek EM, Phillips KA, Chang Y, Henault LE, Selby JV, et al. Prevalence of diagnosed atrial fibrillation in adults: national implications for rhythm management and stroke prevention: the AnTicoagulation and Risk Factors in Atrial Fibrillation (ATRIA) Study. Jama. 2001; 285:2370–5. [PubMed: 11343485]
3. Rosenberg MA, Samuel M, Thosani A, Zimetbaum PJ. Use of a noninvasive continuous monitoring device in the management of atrial fibrillation: a pilot study. Pacing Clin Electrophysiol. 2013; 36:328–33. [PubMed: 23240827]
4. Gladstone DJ, Spring M, Dorian P, Panzov V, Thorpe KE, Hall J, et al. Atrial Fibrillation in Patients with Cryptogenic Stroke. New England Journal of Medicine. 2014; 370:2467–77. [PubMed: 24963566]
5. Turakhia MP, Hoang DD, Zimetbaum P, Miller JD, Froelicher VF, Kumar UN, et al. Diagnostic utility of a novel leadless arrhythmia monitoring device. Am J Cardiol. 2013; 112:520–4. [PubMed: 23672988]
6. Mann H. A method of analyzing the electrocardiogram. Archives of Internal Medicine. 1920; 25:283–94.
7. Wilson FN, Johnston FD. The vectorcardiogram. American Heart Journal. 16:14-28.
8. Tereshchenko LG, Waks JW, Kabir M, Ghafoori E, Shvilkin A, Josephson ME. Analysis of speed, curvature, planarity and frequency characteristics of heart vector movement to evaluate the electrophysiological substrate associated with ventricular tachycardia. Comput Biol Med. 2015; 65:150–60. [PubMed: 25842361]
9. Waks JW, Soliman EZ, Henrikson CA, Sotoodehnia N, Han L, Agarwal SK, et al. Beat-to-beat spatiotemporal variability in the T vector is associated with sudden cardiac death in participants without left ventricular hypertrophy: the Atherosclerosis Risk in Communities (ARIC) Study. J Am Heart Assoc. 2015; 4:e001357. [PubMed: 25600143]
10. Waks JW, Sitlani CM, Soliman EZ, Kabir M, Ghafoori E, Biggs ML, et al. Global Electric Heterogeneity Risk Score for Prediction of Sudden Cardiac Death in the General Population: The Atherosclerosis Risk in Communities (ARIC) and Cardiovascular Health (CHS) Studies. Circulation. 2016; 133:2222–34. [PubMed: 27081116]
11. Kim D-H, Lu N, Ma R, Kim Y-S, Kim R-H, Wang S, et al. Epidermal Electronics. Science. 2011; 333:838–43. [PubMed: 21836009]
12. Sur S, Han L, Tereshchenko LG. Comparison of sum absolute QRST integral, and temporal variability in depolarization and repolarization, measured by dynamic vectorcardiography approach, in healthy men and women. PLoS One. 2013; 8:e57175. [PubMed: 23451181]
13. Tereshchenko LG, Cheng A, Fetics BJ, Marine JE, Spragg DD, Sinha S, et al. Ventricular arrhythmia is predicted by sum absolute QRST integralbut not by QRS width. J Electrocardiol. 2010; 43:548–52. [PubMed: 20832820]
14. Tereshchenko LG, Cheng A, Fetics BJ, Butcher B, Marine JE, Spragg DD, et al. A new electrocardiogram marker to identify patients at low risk for ventricular tachyarrhythmias: sum magnitude of the absolute QRST integral. J Electrocardiol. 2011; 44:208–16. [PubMed: 21093871]
15. Sedaghat G, Ghafoori E, Waks JW, Kabir MM, Shvilkin A, Josephson ME, et al. Quantitative Assessment of Vectorcardiographic Loop Morphology. J Electrocardiol. 2016; 49:154–63. [PubMed: 26826894]

16. Horinaka S, Yamamoto H, Yagi S. Spatial orientation of the vectorcardiogram in patients with myocardial infarction. Jpn Circ J. 1993; 57:109–16. [PubMed: 8450594]
17. Arnaud P, Morlet D, Rubel P. Planarity of the spatial QRS loop. Comparative analysis in normals, infarcts, ventricular hypertrophies, and intraventricular conduction defects. J Electrocardiol. 1989; 22:143–52. [PubMed: 2523464]
18. Bland JM, Altman DG. Statistical methods for assessing agreement between two methods of clinical measurement. Lancet. 1986; 1:307–10. [PubMed: 2868172]
19. Cheung KC, Renaud P, Tanila H, Djupsund K. Flexible polyimide microelectrode array for in vivo recordings and current source density analysis. Biosens Bioelectron. 2007; 22:1783–90. [PubMed: 17027251]
20. Irimia-Vladu M, Troshin PA, Reisinger M, Shmygleva L, Kanbur Y, Schwabegger G, et al. Biocompatible and Biodegradable Materials for Organic Field-Effect Transistors. Advanced Functional Materials. 2010; 20:4069–76.
21. Baumert M, Schmidt M, Zaunseder S, Porta A. Effects of ECG sampling rate on QT interval variability measurement. Biomedical Signal Processing and Control. 2016; 25:159–64.
22. McFee R, Johnston FD. Electrocardiographic leads I. Introduction Circulation. 1953; 8:554–68. [PubMed: 13094793]
23. McFee R, Johnston FD. Electrocardiographic leads II. Analysis Circulation. 1954; 9:255–66. [PubMed: 13127187]
24. McFee R, Johnston FD. Electrocardiographic leads III. Synthesis Circulation. 1954; 9:868–80. [PubMed: 13161116]
25. Geselowitz DB. Electric and Magnetic Field of the Heart. Annual Review of Biophysics and Bioengineering. 1973; 2:37–64.
26. Burger HC, Van Milaan JB. Heart vector and leads. Part II. British Heart Journal. 1947; 9:154–60. [PubMed: 18610067]
27. Malmivuo, J., Plonsey, R. Bioelectromagnetism. Oxford, NY: Oxford University Press; 1995. Vectorcardiographic Lead Systems; p. 290-306.
28. Frank E. General Theory of Heart-Vector Projection. Circulation Research. 1954; 2:258–70. [PubMed: 13161136]
29. Frank E. An accurate, clinically practical system for spatial vectorcardiography. Circulation. 1956; 13:737–49. [PubMed: 13356432]
30. McFee R, Parungao A. An orthogonal lead system for clinical electrocardiography. American Heart Journal. 62:93–100.
31. Barrett PM, Komatireddy R, Haaser S, Topol S, Sheard J, Encinas J, et al. Comparison of 24-hour Holter monitoring with 14-day novel adhesive patch electrocardiographic monitoring. Am J Med. 2014; 127:95.e11-7.
32. Kligfield P, Gettes LS, Bailey JJ, Childers R, Deal BJ, Hancock EW, et al. Recommendations for the Standardization and Interpretation of the Electrocardiogram. Circulation. 2007; 115:1306–24. [PubMed: 17322457]
33. Maier C, Rodler V, Laguna P, Dickhaus H. Dynamic analysis of multi lead ECG recordings for detection and categorization of respiratory events during sleep. Computers in Cardiology. 2007; 34:493–6.
34. Noriega M, Martinez JP, Laguna P, Romero D, Bailon R, Almeida R. Respiration effect on single and multi lead ECG delineation strategies. Conf Proc IEEE Eng Med Biol Soc. 2010:3575–8. [PubMed: 21096831]

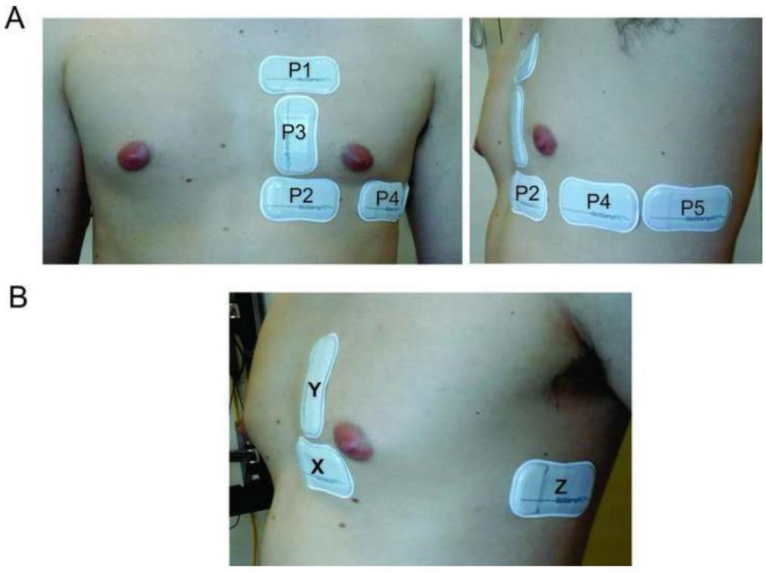

Figure 1.

A: Placement of the patches (P1, P2, P3, P4, P5) on the torso. P1 is placed horizontally over the 3rd intercostal space, between the left parasternal and mid-clavicular line; P2 is placed horizontally over the 5th intercostal space between the left parasternal and mid-clavicular lines; P3 is placed vertically at left parasternal line over the 4th intercostal space; P4 is placed at the horizontal level of P2 at the left anterior axillary line; P5 is placed at the horizontal level of P2 at the left mid-axillary line. B: Optimal configuration of patches. X: placed horizontally over the 5th intercostal space between the left parasternal and mid-clavicular lines; Y: placed vertically at left parasternal line over the 4th intercostal space; Z: placed at the horizontal level of X at the left mid-axillary line.

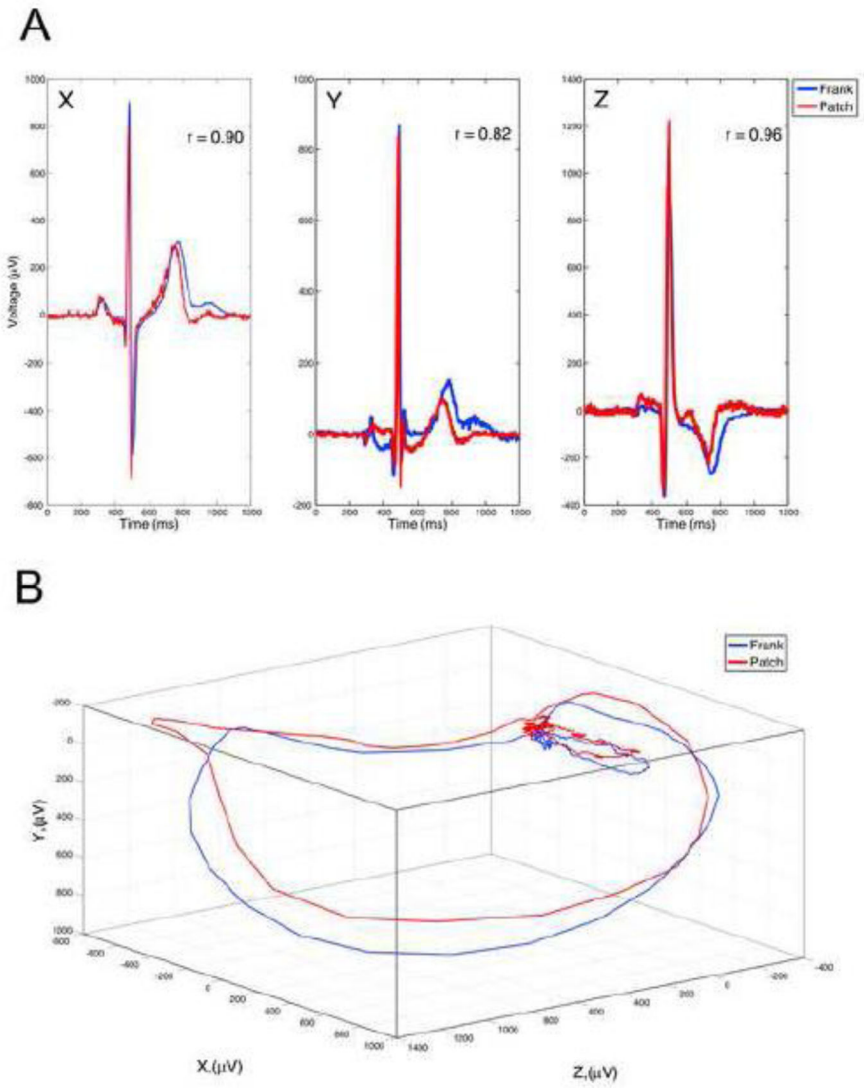

Figure 2.

Representative example of Frank orthogonal X-, Y-, Z- ECG (blue) and patch XYZ ECG leads (red) in a study participant. A: XYZ leads. B: Vectorcardiographic loops

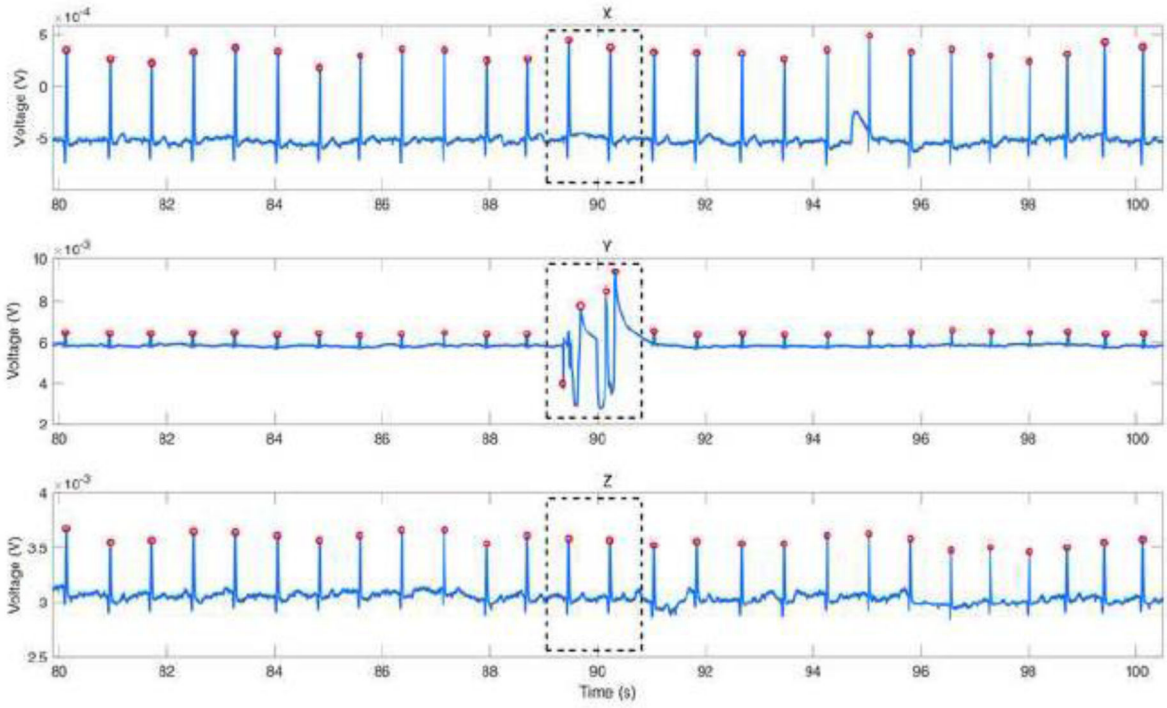

Figure 3.

Representative example of the advantage of multi-lead ECG-analysis. Artefacts on Y-lead could be mislabelled if this would be the only ECG patch used. Simultaneously recorded X and Z leads are free from artefacts at the same time point (dashed box), which increases accuracy of the automated ECG analyses.

Table 1

Clinical characteristics of study participants

Characteristic	Male (n=26)	Female (n=24)
Age, y (SD)	41.98 (16.3)	35.49 (11.8)
White, n(%)	19 (73.1)	19 (79.2)
Heart rate, bpm (SD)	70.73 (14.2)	68.33 (12.6)
Hypertension, n(%)	6 (23.1)	1 (4.2)
Coronary Heart Disease, n(%)	4 (15.4)	0 (0)
Heart Failure, n(%)	4 (15.4)	1 (4.2)
Myocardial Infarction, n(%)	2 (7.7)	0 (0)

Table 2

Reproducibility agreement of VCG characteristics between modified Frank and patch recorded ECGs

Parameter	Modified Frank Leads System (mean±SD)	Orthogonal Patches Leads System (mean±SD)	Lin's concordance	Bias	95% limits of agreement	Bradley- Blackwood F (P)
QT Interval (ms)	394.2±44.4	394.3±44.6	0.998	−0.060	[−6.16;6.04]	0.08 (0.93)
Peak QRS-T angle±SD (°)	49.2±37.3	48.5±38.5	0.989	0.631	[−10.23;11.49]	1.49 (0.24)
Mean QRS-T angle (°)	58.6±35.3	58.9±35.1	0.996	−0.257	[−6.23;5.71]	0.25 (0.78)
Azimuth of Peak QRS Vector(°)	−28.8±40.4	−29.3±41.5	0.988	0.515	[−11.73;12.76]	0.96 (0.39)
Azimuth of Mean QRS Vector (°)	−30.8±46.9	−30.1±47.2	0.997	−0.711	[−7.34;5.92]	1.31 (0.28)
Azimuth of Peak T vector (°)	10.9±61.7	11.2±61.4	0.995	−0.308	[−12.52;11.91]	0.11 (0.90)
Azimuth of Mean T vector (°)	19.4±49.6	19.5±49.0	0.998	−0.098	[−6.08;5.88]	0.87 (0.43)
Azimuth of Peak SVG vector (°)	−17.6±46.7	−17.6±46.6	0.991	0.024	[−12.05;12.09]	0.01 (0.99)
Azimuth of Mean SVG vector (°)	−23.7±40.2	−23.4±40.2	0.997	−0.273	[−6.24;5.70]	0.20 (0.82)
Elevation of Peak QRS vector (°)	57.9±21.7	58.0±23.0	0.967	−0.061	[−11.38;11.26]	1.19 (0.31)
Elevation of Mean QRS vector (°)	60.9±24.1	60.4±23.9	0.992	0.473	[−5.42;6.37]	0.75 (0.48)
Elevation of Peak T vector (°)	65.6±25.2	67.1±27.1	0.971	−1.426	[−13.39;10.54]	4.37 (0.02)
Elevation of Mean T vector (°)	67.4±22.4	67.3±22.6	0.990	0.124	[−6.09;6.34]	0.13 (0.88)
Elevation of Peak SVG vector (°)	57.5±22.3	56.5±23.9	0.971	1.016	[−9.70;11.73]	2.99 (0.06)
Elevation of Mean SVG vector (°)	58.1±22.0	58.4±22.9	0.989	−0.362	[−6.72;5.99]	1.93 (0.16)
QRS Roundness Index	0.51±0.22	0.51±0.22	0.667	−0.001	[−0.36;0.35]	0.001 (0.99)
QRS Loop Thickness (μV)	200.0±126.9	200.0±126.8	1.000	−0.002	[−0.69;0.68]	1.58 (0.22)
QRS Loop Planarity Index	0.87±0.09	0.82±0.17	0.222	0.057	[−0.27;0.38]	18.04 (0.00)
T Loop Roundness Index	0.88±0.71	0.99±0.72	0.895	−0.106	[−0.72;0.51]	2.88 (0.07)
T Loop Thickness (μV)	72.5±41.4	72.5±41.5	1.000	−0.025	[−0.65;0.60]	1.95 (0.15)
SAI QRST (mV.ms)	122.3±35.9	122.2±35.9	1.000	0.041	[−0.32;0.40]	1.30 (0.28)